

REMARKS/ARGUMENTS

Claims 91-111 are active. Page 15 of the specification has been amended to refer to Figs. 28-123. For the convenience of the Examiner, additional description of these figures may be found in the attached "Brief Description of Figs. 28-123". Claims 91-95 find support in the original claims and specification. The ISEApeaks® software is disclosed at least on page 17, line 20 and at the bottom of page 21 of the specification. Sets of peaks having a defined position and area are disclosed on page 18, line 22 of the specification and in original claim 1. Smoothing is disclosed on page 19, lines 9 *ff.* of the specification and in original claim 2. Claims 96-109 track prior claims 46-56. The particular bioinformatic tools in claim 97 are also described on page 19, lines 12-13 of the specification. Claims 110 and 111 find support as described above for claims 91-109 and on pages 20-21 of the specification. No new matter has been added.

The Applicants thank Examiner Negin for the courteous and helpful interview of February 21, 2008. The prior art rejections based on Sotak and Negin were reviewed. Claim language that would avoid the rejections was discussed. The Applicants were urged to provide a brief description of each figure to overcome the objection to the Brief Description of the Drawings. Other revisions to address the indefiniteness and non-statutory subject matter rejections were proposed.

Restriction/Election

The Applicants previously elected with traverse **Group I**, claims 46-56, drawn to a high-throughput analysis method of data sets. Claims 57-90, corresponding to Groups II-VI, have been withdrawn from consideration. The requirement has been made FINAL. The Applicants respectfully request that the claims of the nonelected group(s) which depend from

or otherwise include all the limitations of an allowed elected claim, be rejoined upon an indication of allowability for the elected claim, see MPEP 821.04.

Objections to Preliminary Amendments

The Preliminary Amendment of January 31, 2005 was objected to for not fully describing the drawing changes and for not showing the changes made to the Abstract.

The Attached Letter Submitting Replacement Drawing Sheets provides a description of the changes made to the drawings in greater detail.

The original specification lacked an Abstract, and the Preliminary Amendment merely added one. It is not necessary to provided a marked up copy of a newly added Abstract: 37 C.F.R. §1.121(b)(1)(iii) forbids underlining of an added paragraph. Accordingly, these objections should now be withdrawn.

Rejection—35 U.S.C. §101

Claims 47-52 were rejected under 35 U.S.C. 101, as being directed to non-statutory subject matter. This rejection is moot in view of the cancellation of these claims.

Rejection—35 U.S.C. §112, second paragraph

Claims 46-53 were rejected under 35 U.S.C. 112, second paragraph, as being indefinite. This rejection is moot in view of the cancellation of these claims.

Rejection—35 U.S.C. §101

Claims 46 and 53 were rejected under 35 U.S.C. 101, as being directed to non-statutory subject matter. This rejection is moot in view of the cancellation of these claims.

Rejection—35 U.S.C. §112, second paragraph

Claims 52-56 were rejected under 35 U.S.C. 112, second paragraph, as being indefinite. This rejection is moot in view of the cancellation of these claims.

Rejection—35 U.S.C. §102(b)

Claims 46-50 were rejected under 35 U.S.C. 102(b) as being anticipated by Sotak, et al., *Analyt. Chem.* 55:782. This rejection is moot in view of the cancellation of the prior claims. It would not apply to the new claims because Sotak is directed to a method involving a Fourier Transform and does not disclose a method comprising:

obtaining multiple sets of raw data from a primary source, wherein each data set has peaks having a defined position and area,

smoothing the peaks in each data set based on one or more user defined parameters using the ISEApeaks[®] software, and

storing each smoothed data set in a data file.

Rejection—35 U.S.C. §102(b)

Claims 446 and 49-56 were rejected under 35 U.S.C. 102(b) as being anticipated by Faure, et al., *J. Immunol.* 163:6511. This rejection is moot in view of the cancellation of the rejected claims. It would not apply to the new claims, because Faure does not disclose a method comprising:

obtaining multiple sets of raw data from a primary source, wherein each data set has peaks having a defined position and area,

smoothing the peaks in each data set based on one or more user defined parameters using the ISEApeaks[®] software, and

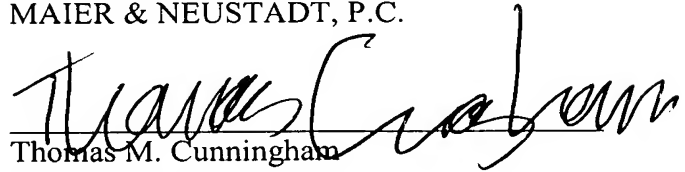
storing each smoothed data set in a data file.

Conclusion

In view of the amendments and remarks above, the Applicants respectfully submit that this application is now in condition for allowance. An early notice to that effect is earnestly solicited.

Respectfully submitted,

OBLON, SPIVAK, McCLELLAND,
MAIER & NEUSTADT, P.C.

A handwritten signature in black ink, appearing to read "Thomas M. Cunningham", is written over a horizontal line.

Thomas M. Cunningham
Registration No. 45,394

Customer Number
22850

Tel: (703) 413-3000
Fax: (703) 413 -2220
(OSMMN 06/04)

BRIEF DESCRIPTION OF FIGS. 28-123

Fig 28: ISEApeaks analysis of TCRalpha and TCRbeta repertoire in seven-week-old female BALB/C mice which received an injection at the level of footpads of the LACK protein, or the LACKp (156-173)peptide, with or without treatment by an anti-IL-2 antibody. Every group of mice includes 5 individuals. Five additional mice received an injection of DMEM buffer and serve as controls. The draining lymph nodes were taken 16 hours after injection. Total ARN was extracted and reverse-transcribed into cDNA. The Immunoscope technique was applied to describe the diversity of $V\alpha C\alpha$ and $V\beta C\beta$ repertoire, for $V\beta 4$, $V\beta 8.1$, $V\alpha 2$, $V\alpha 8$ and $V\alpha 15$ TCRV-C combinations. (A) color-coded array and (B) numerical values of repertoire disturbance. “Gorochov perturbation” tables representing the global variability for each $V\alpha$ - $C\alpha$, $V\beta$ - $C\beta$ or $V\beta$ - $J\beta$ profile of every sample with regard to the average variability measured for the control group (group n°1 - DMEM injection); (C) drawarray and (D) numerical values of repertoire disturbance normalized against oligoscores. “Gorochov perturbation” tables normalized by the “Oligoscore” values: for each individual and each $V\alpha$ - $C\alpha$ / $V\beta$ - $C\beta$ / $V\beta$ - $J\beta$ combination, the value of “Gorochov perturbation” of the individual was normalized by the ratio of the maximum Oligoscore for the $V\alpha$ - $C\alpha$ / $V\beta$ - $C\beta$ / $V\beta$ - $J\beta$ combination of the group considered by the maximum Oligoscore for the $V\alpha$ - $C\alpha$ / $V\beta$ - $C\beta$ / $V\beta$ - $J\beta$ combination measured for the control group.

Fig 29: Table “DataAnalyser DA” created with ISEApeaks to prepare the extraction of the data through the various gels. It is at this level that the distribution of samples in groups is indicated. Samples are the same as in Fig 28.

Fig 30: ISEApeaks analysis of (A) Drawarray and numerical values of $V\beta 4$ - $C\beta$ and $V\beta 8.1$ - $C\beta$ disturbance normalized against Oligoscores and (B) Drawarray and numerical values of $V\beta 4$ - $C\beta$ and $V\beta 8.1$ - $C\beta$ disturbance. Repertoire disturbance analysis of 3/5 samples for each group as described in Fig 28.

Fig 31: Table “DataAnalyser DA” created with ISEApeaks to prepare the extraction of the data through the various gels for $V\beta 4$ - $C\beta$ and $V\beta 4$ - $C\beta$ analysis It is at this level that the distribution of samples in groups is indicated. Samples are the same as in Fig 30.

Fig 32: “Gorochov perturbation” tables representing the global variability for each $V\beta 4$ - $J\beta$ profile of every sample analyzed with regard to the average variability measured for

the control group (group n°1 - DMEM injection). (A) Drawarray and numerical values of V β 4-J β disturbance and (B) Drawarray and numerical values of V β 4-J β disturbance normalized against Oligoscores. Samples are the same as in Fig 30.

Fig 33: Table “DataAnalyser DA” created with ISEApeaks to prepare the extraction of the data through the various gels for V β 4-J β analysis It is at this level that the distribution of samples in groups is indicated. Samples are the same as in Fig 30.

Fig 34: “Gorochov perturbation” tables representing the global variability for each V β 8.1-J β profile of every sample analyzed with regard to the average variability measured for the control group (group n°1 - DMEM injection). (A) Drawarray and numerical values of V β 8.1-J β disturbance normalized against Oligoscores and (B) Drawarray and numerical values of V β 8.1-J β disturbance. Samples are the same as in Fig 30.

Fig 35: Table “DataAnalyser DA” created with ISEApeaks to prepare the extraction of the data through the various gels for V β 8.1-J β analysis It is at this level that the distribution of samples in groups is indicated. Samples are the same as in Fig 30.

Fig 36: Perturbation of the CD4⁺ and CD8⁺ T lymphocyte repertoires during Leishmania infection in a murine experimental model. Table “DataAnalyser DA” created with ISEApeaks to prepare the extraction of the data through the various gels for V β -C β analysis of Spleen CD4⁺ samples. It is at this level that the distribution of samples in groups is indicated. This study was carried out with wild-derived PWK inbred mice which was selected as a new promising model for human *Leishmania major* infection since the clinical and biological features of PWK mice parallels those observed in humans. PWK mice were infected by *Leishmania major* in footpads. 7, 20 and 27 weeks after infection groups of 6 mice were sacrificed. Lymphocyte cell suspensions were prepared from draining lymph nodes (G) and spleen (R) and sorted into CD4⁺ and CD8⁺ sub-populations. Six additional mice were sacrificed just after infection and serve as controls. Total ARN was extracted and reverse-transcribed into cDNA. The Immunoscope technique was applied to describe the diversity of V β C β repertoires. In this table Spleen CD8⁺ samples 0, 7, 20 and 27 weeks after infection are provided.

Fig 37: Perturbation of the CD4⁺ and CD8⁺ T lymphocyte repertoires during Leishmania infection in a murine experimental model. Synthetic graphs for 7 and 27 weeks

Spleen CD4⁺ samples were drawn to represent the “Gorochov perturbation” of V β -C β combinations for which the “Gorochov perturbation” is statistically different than control mice. Samples are the same as in Fig 36.

Fig 38: Perturbation of the CD4⁺ and CD8⁺ T lymphocyte repertoires during Leishmania infection in a murine experimental model. “Gorochov perturbation” (G1%) tables were generated to represent the global variability for each V β -C β profile of every sample with regard to the average variability measured for the control group. “Gorochov perturbation” were then computed by ANOVA for determining whether groups are statistically different based on their repertoire diversity. Spleen CD4⁺ samples analyzed are the same as in Fig 36.

Fig 39: Perturbation of the CD4⁺ and CD8⁺ T lymphocyte repertoires during Leishmania infection in a murine experimental model. Significant Oligoscore (Score d’oligoclonalité β V) identified in the Spleen CD4⁺ samples (Rate-CD4⁺) 7 weeks (7 semaines post-infection) or 27 weeks after infection (27 semaines post-infection). “Oligoscore” tables were generated for each group as described in Fig 36 indicating the possible presence of recurrent oligoclonal peaks indicative of recurrent clonal lymphocyte expansions within a group. Heuristically, the threshold value corresponds to the maximal “Oligoscore” value of the control group for which no significant expansion is expected. Only significant expansion are shown here.

Fig 40: Perturbation of the CD4⁺ and CD8⁺ T lymphocyte repertoires during Leishmania infection in a murine experimental model. “Expression level” tables (R%) were generated to indicate the level of expression each V β -C β profile of every sample. Note that the experimental condition used here are not quantitative so that this value is only indicative when a major change is observed. Spleen CD4⁺ samples analyzed are the same as in Fig 36.

Fig 41: Perturbation of the CD4⁺ and CD8⁺ T lymphocyte repertoires during Leishmania infection in a murine experimental model. Table “DataAnalyser DA” created with ISEApeaks to prepare the extraction of the data through the various gels for V β -C β analysis of Lymph Node CD4⁺ samples. Sample description is the same as in Fig 36.

Fig 42: Perturbation of the CD4⁺ and CD8⁺ T lymphocyte repertoires during Leishmania infection in a murine experimental model. Synthetic graphs for 7 and 27 weeks Lymph Node CD4⁺ samples were drawn to represent the “Gorochov perturbation” of V β -C β

combinations for which the “Gorochov perturbation” is statistically different than control mice. Samples are the same as in Fig 36.

Fig 43: Perturbation of the CD4+ and CD8+ T lymphocyte repertoires during Leishmania infection in a murine experimental model. “Gorochov perturbation” (G1%) tables were generated to represent the global variability for each V β -C β profile of every sample with regard to the average variability measured for the control group. “Gorochov perturbation” were then computed by ANOVA for determining whether groups are statistically different based on their repertoire diversity. Lymph node CD4+ samples analyzed are the same as in Fig 36.

Fig 44: Perturbation of the CD4+ and CD8+ T lymphocyte repertoires during Leishmania infection in a murine experimental model. Significant Oligoscore (Score d’oligoclonalité β V) identified in the Lymph nodes CD4+ samples (GG-CD4+) 7 weeks (7 semaines post-infection) or 27 weeks after infection (27 semaines post-infection). “Oligoscore” tables were generated for each group as described in Fig 36 indicating the possible presence of recurrent oligoclonal peaks indicative of recurrent clonal lymphocyte expansions within a group. Heuristically, the threshold value corresponds to the maximal “Oligoscore” value of the control group for which no significant expansion is expected. Only significant expansion are shown here.

Fig 45: Perturbation of the CD4+ and CD8+ T lymphocyte repertoires during Leishmania infection in a murine experimental model. “Expression level” tables (R%) were generated to indicate the level of expression each V β -C β profile of every sample. Note that the experimental condition used here are not quantitative so that this value is only indicative when a major change is observed. Lymph node CD4+ samples analyzed are the same as in Fig 36.

Fig 46: Perturbation of the CD4+ and CD8+ T lymphocyte repertoires during Leishmania infection in a murine experimental model. Table “DataAnalyser DA” created with ISEApeaks to prepare the extraction of the data through the various gels for V β -C β analysis of Lymph Node CD8+ samples. Sample description is the same as in Fig 36.

Fig 47: Perturbation of the CD4+ and CD8+ T lymphocyte repertoires during Leishmania infection in a murine experimental model. Synthetic graphs for 7 and 27 weeks Lymph Node CD8+ samples were drawn to represent the “Gorochov perturbation” of V β -C β

combinations for which the “Gorochov perturbation” is statistically different than control mice. Samples are the same as in Fig 36.

Fig 48: Perturbation of the CD4⁺ and CD8⁺ T lymphocyte repertoires during Leishmania infection in a murine experimental model. “Gorochov perturbation” (G1%) tables were generated to represent the global variability for each V β -C β profile of every sample with regard to the average variability measured for the control group. “Gorochov perturbation” were then computed by ANOVA for determining whether groups are statistically different based on their repertoire diversity. Lymph node CD8⁺ samples analyzed are the same as in Fig 36.

Fig 49: Perturbation of the CD4⁺ and CD8⁺ T lymphocyte repertoires during Leishmania infection in a murine experimental model. Significant Oligoscore (Score d’oligoclonalité β V) identified in the Lymph nodes CD8⁺ samples (GG-CD8⁺) 7 weeks (7 semaines post-infection) or 27 weeks after infection (27 semaines post-infection). “Oligoscore” tables were generated for each group as described in Fig 36 indicating the possible presence of recurrent oligoclonal peaks indicative of recurrent clonal lymphocyte expansions within a group. Heuristically, the threshold value corresponds to the maximal “Oligoscore” value of the control group for which no significant expansion is expected. Only significant expansion are shown here.

Fig 50: Perturbation of the CD4⁺ and CD8⁺ T lymphocyte repertoires during Leishmania infection in a murine experimental model. “Expression level” tables (R%) were generated to indicate the level of expression each V β -C β profile of every sample. Note that the experimental condition used here are not quantitative so that this value is only indicative when a major change is observed. Lymph node CD8⁺ samples analyzed are the same as in Fig 36.

Fig 51: Perturbation of the CD4⁺ and CD8⁺ T lymphocyte repertoires during Leishmania infection in a murine experimental model. Table “DataAnalyser DA” created with ISEApeaks to prepare the extraction of the data through the various gels for V β -C β analysis of Spleen CD8⁺ samples. Sample description is the same as in Fig 36.

Fig 52: Perturbation of the CD4⁺ and CD8⁺ T lymphocyte repertoires during Leishmania infection in a murine experimental model. Synthetic graphs for 7 and 27 weeks Spleen CD8⁺ samples were drawn to represent the “Gorochov perturbation” of V β -C β

combinations for which the “Gorochov perturbation” is statistically different than control mice. Samples are the same as in Fig 36.

Fig 53: Perturbation of the CD4+ and CD8+ T lymphocyte repertoires during Leishmania infection in a murine experimental model. “Gorochov perturbation” (G1%) tables were generated to represent the global variability for each V β -C β profile of every sample with regard to the average variability measured for the control group. “Gorochov perturbation” were then computed by ANOVA for determining whether groups are statistically different based on their repertoire diversity. Spleen CD8+ samples analyzed are the same as in Fig 36.

Fig 54: Perturbation of the CD4+ and CD8+ T lymphocyte repertoires during Leishmania infection in a murine experimental model. Significant Oligoscore (Score d’oligoclonalité β V) identified in the Spleen CD8+ samples (Rate-CD8+) 7 weeks (7 semaines post-infection) or 27 weeks after infection (27 semaines post-infection). “Oligoscore” tables were generated for each group as described in Fig 36 indicating the possible presence of recurrent oligoclonal peaks indicative of recurrent clonal lymphocyte expansions within a group. Heuristically, the threshold value corresponds to the maximal “Oligoscore” value of the control group for which no significant expansion is expected. Only significant expansion are shown here.

Fig 55: Perturbation of the CD4+ and CD8+ T lymphocyte repertoires during Leishmania infection in a murine experimental model. “Expression level” tables (R%) were generated to indicate the level of expression each V β -C β profile of every sample. Note that the experimental condition used here are not quantitative so that this value is only indicative when a major change is observed. Spleen CD8+ samples analyzed are the same as in Fig 36.

Fig 56: Kinetic of perturbation of $\alpha\beta$ T lymphocyte repertoires in a murine experimental model of cerebral malaria. “DataAnalyser DA” table created with ISEApeaks to prepare the extraction of the data through the various gels. It is at this level that the distribution of samples in groups is indicated. This study was carried out with 2-month-old B10.D2 mice. They were infected by intraperitoneal injection of 10^6 *Plasmodium berghei* ANKA clone 1.49L parasitized red blood cells. We constituted six groups of mice: J3, J4, J5 and J6 groups (3, 4, 5 and 6 days after infection, respectively). J3 group included 5 mice when J4, J5 and J6 groups included 10 mice. The TSP group included 20 infected individuals and was used to follow the onset of cerebral malaria (CM). Parasitemia was systematically

assessed before sacrificing the mice to confirm infection. Five additional mice were not infected and served as controls (TN group). Blood, spleen and brain were collected for each individual. For the TSP group, collection was done on the onset of CM clinical signs as assessed by paralysis, deviation of the head, respiratory troubles. For the TN group, collection was done on day 14 of the experiment. Total RNA was extracted and reverse-transcribed into cDNA. The Immunoscope technique was applied to describe the diversity of V β -C β repertoire, for all the 23 V β TCRBV-BC combinations.

Fig 57: Kinetic of perturbation of $\alpha\beta$ T lymphocyte repertoires in a murine experimental model of cerebral malaria. "Gorochov perturbation" table representing the global variability for each V β -C β profile of every sample with regard to the average variability measured for the control group (non-infected TN group). Samples analyzed are the same as in Fig 56.

Fig 58: Kinetic of perturbation of $\alpha\beta$ T lymphocyte repertoires in a murine experimental model of cerebral malaria. "Gorochov perturbation" tables normalized by the "Oligoscore" values: for each individual and each V β -C β combination, the value of "Gorochov perturbation" of the individual was normalized by the ratio of the maximum Oligoscore for the V β -C β combination of the group considered by the maximum Oligoscore for the V β -C β combination measured for the control group. Samples analyzed are the same as in Fig 56.

Fig 59: Kinetic of perturbation of $\alpha\beta$ T lymphocyte repertoires in a murine experimental model of cerebral malaria. Statistical ANOVA analysis of V β 1 "Gorochov perturbation" values as described in Fig 57 to assess the statistical differences between the experimental groups analyzed for cerebral malaria (CM), day 3 (J3), day 4 (J4), day 5 (J5), day 6 (J6) and uninfected (TN) spleen (S) and blood (P) samples. (A) ANOVA table presenting group (groupe), residual (residus), sum of squares (somme des carrés), mean square (carré moyen), F (valeur de F), p (valeur de p), lambda and power (puissance) statistics; (B) Table of means (tableau des moyennes), group effect indicating the number (nombre), average (moyenne), standard deviation (Dev. Std) and standard error (Err. Std) of samples; (C) Graph of interactions, group effect (Graphe des interactions; effet groupe); (D) Fisher's PLSD test (PLSD de Fisher), group effect (effet groupe), significance level (niveau de significativité) 5%, "S" indicates a significant difference; (E-H) same as in (A-D) for V β 2.

Fig 60: Kinetic of perturbation of $\alpha\beta$ T lymphocyte repertoires in a murine experimental model of cerebral malaria. Statistical ANOVA analysis of V β 3 (A-D) and V β 4 (E-H) "Gorochov perturbation" values as described in Fig 57. Same legend as in Fig 59.

Fig 61: Kinetic of perturbation of $\alpha\beta$ T lymphocyte repertoires in a murine experimental model of cerebral malaria. Statistical ANOVA analysis of V β 5.1 (A-D) and V β 5.2 (E-H) "Gorochov perturbation" values as described in Fig 57. Same legend as in Fig 59.

Fig 62: Kinetic of perturbation of $\alpha\beta$ T lymphocyte repertoires in a murine experimental model of cerebral malaria. Statistical ANOVA analysis of V β 6 (A-D) and V β 7 (E-H) "Gorochov perturbation" values as described in Fig 57. Same legend as in Fig 59.

Fig 63: Kinetic of perturbation of $\alpha\beta$ T lymphocyte repertoires in a murine experimental model of cerebral malaria. Statistical ANOVA analysis of V β 8.1 (A-D) and V β 8.2 (E-H) "Gorochov perturbation" values as described in Fig 57. Same legend as in Fig 59.

Fig 64: Kinetic of perturbation of $\alpha\beta$ T lymphocyte repertoires in a murine experimental model of cerebral malaria. Statistical ANOVA analysis of V β 8.3 (A-D) and V β 9 (E-H) "Gorochov perturbation" values as described in Fig 57. Same legend as in Fig 59.

Fig 65: Kinetic of perturbation of $\alpha\beta$ T lymphocyte repertoires in a murine experimental model of cerebral malaria. Statistical ANOVA analysis of V β 10 (A-D) and V β 11 (E-H) "Gorochov perturbation" values as described in Fig 57. Same legend as in Fig 59.

Fig 66: Kinetic of perturbation of $\alpha\beta$ T lymphocyte repertoires in a murine experimental model of cerebral malaria. Statistical ANOVA analysis of V β 12 (A-D) and V β 13 (E-H) "Gorochov perturbation" values as described in Fig 57. Same legend as in Fig 59.

Fig 67: Kinetic of perturbation of $\alpha\beta$ T lymphocyte repertoires in a murine experimental model of cerebral malaria. Statistical ANOVA analysis of V β 14 (A-D) and

V β 15 (E-H) “Gorochov perturbation” values as described in Fig 57. Same legend as in Fig 59.

Fig 68: Kinetic of perturbation of $\alpha\beta$ T lymphocyte repertoires in a murine experimental model of cerebral malaria. Statistical ANOVA analysis of V β 16 (A-D) and V β 18 (E-H) “Gorochov perturbation” values as described in Fig 57. Same legend as in Fig 59.

Fig 69: Kinetic of perturbation of $\alpha\beta$ T lymphocyte repertoires in a murine experimental model of cerebral malaria. Statistical ANOVA analysis of V β 20 (A-D) “Gorochov perturbation” values as described in Fig 57. Same legend as in Fig 59.

Fig 70: Kinetic of perturbation of $\alpha\beta$ T lymphocyte repertoires in a murine experimental model of cerebral malaria. Statistical ANOVA analysis of V β 1 (A-D) and V β 2 (E-H) “Gorochov perturbation” values. Similarly to the analysis described in Fig 59, another ANOVA analysis was performed based on three sets of individuals only: one set comprising controls, J3 and J4 groups; a second set corresponding to J5 group; a third set comprising J6 and TSP groups. Legend is the same as in Fig 59.

Fig 71: Kinetic of perturbation of $\alpha\beta$ T lymphocyte repertoires in a murine experimental model of cerebral malaria. Statistical ANOVA analysis of V β 3 (A-D) and V β 4 (E-H) “Gorochov perturbation” values as described in Fig 70. Legend is the same as in Fig 59.

Fig 72: Kinetic of perturbation of $\alpha\beta$ T lymphocyte repertoires in a murine experimental model of cerebral malaria. Statistical ANOVA analysis of V β 5.1 (A-D) and V β 5.2 (E-H) “Gorochov perturbation” values as described in Fig 70. Legend is the same as in Fig 59.

Fig 73: Kinetic of perturbation of $\alpha\beta$ T lymphocyte repertoires in a murine experimental model of cerebral malaria. Statistical ANOVA analysis of V β 6 (A-D) and V β 7 (E-H) “Gorochov perturbation” values as described in Fig 70. Legend is the same as in Fig 59.

Fig 74: Kinetic of perturbation of $\alpha\beta$ T lymphocyte repertoires in a murine experimental model of cerebral malaria. Statistical ANOVA analysis of V β 8.1 (A-D) and V β 8.2 (E-H) “Gorochov perturbation” values as described in Fig 70. Legend is the same as in Fig 59.

Fig 75: Kinetic of perturbation of $\alpha\beta$ T lymphocyte repertoires in a murine experimental model of cerebral malaria. Statistical ANOVA analysis of V β 8.3 (A-D) and V β 9 (E-H) “Gorochov perturbation” values as described in Fig 70. Legend is the same as in Fig 59.

Fig 76: Kinetic of perturbation of $\alpha\beta$ T lymphocyte repertoires in a murine experimental model of cerebral malaria. Statistical ANOVA analysis of V β 10 (A-D) and V β 11 (E-H) “Gorochov perturbation” values as described in Fig 70. Legend is the same as in Fig 59.

Fig 77: Kinetic of perturbation of $\alpha\beta$ T lymphocyte repertoires in a murine experimental model of cerebral malaria. Statistical ANOVA analysis of V β 12 (A-D) and V β 13 (E-H) “Gorochov perturbation” values as described in Fig 70. Legend is the same as in Fig 59.

Fig 78: Kinetic of perturbation of $\alpha\beta$ T lymphocyte repertoires in a murine experimental model of cerebral malaria. Statistical ANOVA analysis of V β 14 (A-D) and V β 15 (E-H) “Gorochov perturbation” values as described in Fig 70. Legend is the same as in Fig 59.

Fig 79: Kinetic of perturbation of $\alpha\beta$ T lymphocyte repertoires in a murine experimental model of cerebral malaria. Statistical ANOVA analysis of V β 16 (A-D) and V β 18 (E-H) “Gorochov perturbation” values as described in Fig 70. Legend is the same as in Fig 59.

Fig 80: Kinetic of perturbation of $\alpha\beta$ T lymphocyte repertoires in a murine experimental model of cerebral malaria. Statistical ANOVA analysis of V β 20 (A-B) “Gorochov perturbation” values as described in Fig 70. Legend is the same as in Fig 59.

Fig 81: Effect of vaccination with irradiated *Plasmodium yoelii* sporozoites on the repertoire of $\alpha\beta$ T lymphocytes in a murine model of malaria. "DataAnalyser DA" table created with ISEApeaks to prepare the extraction of the data through the various gels. It is at this level that the distribution of samples in groups is indicated. This study was carried out with C57BL/6 mice. Mice were constituted into groups as follows: 1. A group of mice was immunized three times with irradiated *Plasmodium yoelii* sporozoites in order to induce protection to *P. yoelii* infection (I3*). 2. A group of mice was immunized three times with irradiated *Plasmodium yoelii* sporozoites in order to induce protection to *P. yoelii* infection and later challenged with infectious *Plasmodium yoelii* sporozoites (I3*S). 3. A group of mice was challenged with infectious *Plasmodium yoelii* sporozoites (S). 4. An additional group of unmanipulated mice served as controls (T). One week after challenge, spleen (R) and liver (F) were collected and lymphocyte suspensions were prepared. Total ARN was extracted and reverse-transcribed into cDNA. The Immunoscope technique was applied to describe the diversity of V β -C β repertoire, for all the 23 V β TCRBV-BC combinations. Spleen samples are assembled in Fig 81.

Fig 82: Effect of vaccination with irradiated *Plasmodium yoelii* sporozoites on the repertoire of $\alpha\beta$ T lymphocytes in a murine model of malaria. "Oligoscore" tables for each group indicating the possible presence of recurrent oligoclonal peaks indicative of recurrent clonal lymphocyte expansions within a group. Heuristically, the threshold value corresponds to the maximal "Oligoscore" value of the control group for which no significant expansion is expected. This table compares the Spleen samples (RT vs. RS vs. R3* vs. R3*S) as described in Fig 81.

Fig 83: Effect of vaccination with irradiated *Plasmodium yoelii* sporozoites on the repertoire of $\alpha\beta$ T lymphocytes in a murine model of malaria. "DataAnalyser DA" table created with ISEApeaks to prepare the extraction of the data through the various gels. It is at this level that the distribution of samples in groups is indicated. Liver (F) samples as described in Fig 81 are assembled in this table.

Fig 84: Effect of vaccination with irradiated *Plasmodium yoelii* sporozoites on the repertoire of $\alpha\beta$ T lymphocytes in a murine model of malaria. "Oligoscore" tables for each group indicating the possible presence of recurrent oligoclonal peaks indicative of recurrent clonal lymphocyte expansions within a group. Heuristically, the threshold value corresponds to the maximal "Oligoscore" value of the control group for which no significant expansion is

expected. This table compares the Liver samples (FT vs. FS vs. F3* vs. F3*S) as described in Fig 81.

Fig 85: Effect of vaccination with irradiated *Plasmodium yoelii* sporozoites on the repertoire of $\alpha\beta$ T lymphocytes in a murine model of malaria. List of samples analyzed as described in Fig 81.

Fig 86: Effect of vaccination with irradiated *Plasmodium yoelii* sporozoites on the repertoire of $\alpha\beta$ T lymphocytes in a murine model of malaria. Average “Gorochov perturbation” ($\mu\text{IndivDVb}$) graph comparing the perturbation between organs Spleen (Rate) & Liver (F) and experimental groups (T, S, I3* & I3*S) as described in Fig 81.

Fig 87: Effect of vaccination with irradiated *Plasmodium yoelii* sporozoites on the repertoire of $\alpha\beta$ T lymphocytes in a murine model of malaria. Average “Gorochov perturbation” (μDVB) graph comparing the perturbation between experimental groups (FT, FS, FI3* & FI3*S) in the Liver (Foie) as described in Fig 81.

Fig 88: Effect of vaccination with irradiated *Plasmodium yoelii* sporozoites on the repertoire of $\alpha\beta$ T lymphocytes in a murine model of malaria. Average “Gorochov perturbation” (μDVB) graph comparing the perturbation between experimental groups (RT, RS, RI3* & RI3*S) in the Spleen (Rate) as described in Fig 81.

Fig 89: Effect of vaccination with irradiated *Plasmodium yoelii* sporozoites on the repertoire of $\alpha\beta$ T lymphocytes in a murine model of malaria. Gorochov perturbation data was analyzed for $V\beta 1\text{-C}\beta$ combination by analysis of variance (ANOVA) in order to identify statistically significant differences between groups as described in Fig 81. (A) ANOVA table presenting group (groupe), organ (organe), group + organ (groupe + organe), residual (residus), sum of squares (somme des carrés), mean square (carré moyen), F (valeur de F), p (valeur de p), lambda and power (puissance) statistics; (B) Table of means (tableau des moyennes), group+organ effect indicating the number (nombre), average (moyenne), standard deviation (Dev. Std) and standard error (Err. Std) of samples; (C) Fisher’s PLSD test (PLSD de Fisher), group effect (effet groupe), significance level (niveau de significativité) 5%, “S” indicates a significant difference; (D) Fisher’s PLSD test (PLSD de Fisher), organ effect (effet organe), significance level (niveau de significativité) 5%, “S” indicates a

significant difference; Graph of interactions, group + organ effect (Graphe des interactions; effet groupe + organe); (E-H) same as in (A-D) for V β 2.

Fig 90: Effect of vaccination with irradiated Plasmodium yoelii sporozoites on the repertoire of $\alpha\beta$ T lymphocytes in a murine model of malaria. Statistical ANOVA analysis of V β 5.1 (A-D) and V β 5.2 (E-H) "Gorochov perturbation" values as described in Fig 81. Legend is the same as in Fig 89.

Fig 91: Effect of vaccination with irradiated Plasmodium yoelii sporozoites on the repertoire of $\alpha\beta$ T lymphocytes in a murine model of malaria. Statistical ANOVA analysis of V β 8.1 (A-D) and V β 8.2 (E-H) "Gorochov perturbation" values as described in Fig 81. Legend is the same as in Fig 89.

Fig 92: Effect of vaccination with irradiated Plasmodium yoelii sporozoites on the repertoire of $\alpha\beta$ T lymphocytes in a murine model of malaria. Statistical ANOVA analysis of V β 10 (A-D) and V β 11 (E-H) "Gorochov perturbation" values as described in Fig 81. Legend is the same as in Fig 89.

Fig 93: Effect of vaccination with irradiated Plasmodium yoelii sporozoites on the repertoire of $\alpha\beta$ T lymphocytes in a murine model of malaria. Statistical ANOVA analysis of V β 14 (A-D) and V β 15 (E-H) "Gorochov perturbation" values as described in Fig 81. Legend is the same as in Fig 89.

Fig 94: Effect of vaccination with irradiated Plasmodium yoelii sporozoites on the repertoire of $\alpha\beta$ T lymphocytes in a murine model of malaria. Statistical ANOVA analysis of V β 20 (A-D) "Gorochov perturbation" values as described in Fig 81. Legend is the same as in Fig 89.

Fig 95: Effect of vaccination with irradiated Plasmodium yoelii sporozoites on the repertoire of $\alpha\beta$ T lymphocytes in a murine model of malaria. Statistical ANOVA analysis of "Gorochov perturbation" values as described in Fig 81. (A) summary table showing the group (Effet groupe OUI) and organ (Effet organe OUI) effects or not (NON) for the different V β -C β combinations. In parentheses are indicated groups for which significant Oligoscores are found for the corresponding V β . ANOVA graphs of interactions, group + organ effect

(Graphe des interactions; effet groupe + organe) for V β 8.3 (B), V β 3 (C), V β 13 (D), V β 14 (E), V β 20 (F), V β 12 (G).

Fig 96: Effect of vaccination with irradiated *Plasmodium yoelii* sporozoites on the repertoire of $\alpha\beta$ T lymphocytes in a murine model of malaria. Heuristic tree of decision for V β -C β disturbance analysis.

Fig 97: Effect of vaccination with irradiated *Plasmodium yoelii* sporozoites on the repertoire of $\alpha\beta$ T lymphocytes in a murine model of malaria. Principle Component Analysis followed by Discriminant Analysis on samples as described in Fig 81 was performed in order to determine how many groups can be distinguished based on peak percentage information. The plot of data according to the first five factors is shown.

Fig 98: Effect of vaccination with irradiated *Plasmodium yoelii* sporozoites on the repertoire of $\alpha\beta$ T lymphocytes in a murine model of malaria. Principle Component Analysis followed by Discriminant Analysis on samples as described in Fig 81 was performed in order to determine how many groups can be distinguished based on peak percentage information. This figure presents the numerical values obtained after computation of the Vb-Cb spectratype data.

Fig 99: Effect of vaccination with irradiated *Plasmodium yoelii* sporozoites on the repertoire of $\alpha\beta$ T lymphocytes in a murine model of malaria. Followed from Fig 98.

Fig 100: Effect of vaccination with irradiated *Plasmodium yoelii* sporozoites on the repertoire of $\alpha\beta$ T lymphocytes in a murine model of malaria. Followed from Fig 99.

Fig 101: Effect of vaccination with irradiated *Plasmodium yoelii* sporozoites on the repertoire of $\alpha\beta$ T lymphocytes in a murine model of malaria. Followed from Fig 100.

Fig 102: Effect of vaccination with irradiated *Plasmodium yoelii* sporozoites on the repertoire of $\alpha\beta$ T lymphocytes in a murine model of malaria. Followed from Fig 101.

Fig 103: Effect of vaccination with irradiated *Plasmodium yoelii* sporozoites on the repertoire of $\alpha\beta$ T lymphocytes in a murine model of malaria. Followed from Fig 102.

Fig 104: Effect of vaccination with irradiated *Plasmodium yoelii* sporozoites on the repertoire of $\alpha\beta$ T lymphocytes in a murine model of malaria. Followed from Fig 103.

Fig 105: Effect of vaccination with irradiated *Plasmodium yoelii* sporozoites on the repertoire of $\alpha\beta$ T lymphocytes in a murine model of malaria. Followed from Fig 104.

Fig 106: Effect of vaccination with irradiated *Plasmodium yoelii* sporozoites on the repertoire of $\alpha\beta$ T lymphocytes in a murine model of malaria. Followed from Fig 105.

Fig 107: Effect of vaccination with irradiated *Plasmodium yoelii* sporozoites on the repertoire of $\alpha\beta$ T lymphocytes in a murine model of malaria. Followed from Fig 106. (B) table of Variance explained by components & Percent of total variance explained. (C) screen plot of Eigen values.

Fig 108: Effect of vaccination with irradiated *Plasmodium yoelii* sporozoites on the repertoire of $\alpha\beta$ T lymphocytes in a murine model of malaria. Followed from Fig 107. Table presents coefficients for standardized factor scores.

Fig 109: Effect of vaccination with irradiated *Plasmodium yoelii* sporozoites on the repertoire of $\alpha\beta$ T lymphocytes in a murine model of malaria. Followed from Fig 108.

Fig 110: Effect of vaccination with irradiated *Plasmodium yoelii* sporozoites on the repertoire of $\alpha\beta$ T lymphocytes in a murine model of malaria. Followed from Fig 109.

Fig 111: Effect of vaccination with irradiated *Plasmodium yoelii* sporozoites on the repertoire of $\alpha\beta$ T lymphocytes in a murine model of malaria. Followed from Fig 110.

Fig 112: Effect of vaccination with irradiated *Plasmodium yoelii* sporozoites on the repertoire of $\alpha\beta$ T lymphocytes in a murine model of malaria. Followed from Fig 111.

Fig 113: Effect of vaccination with irradiated *Plasmodium yoelii* sporozoites on the repertoire of $\alpha\beta$ T lymphocytes in a murine model of malaria. Followed from Fig 112.

Fig 114: Effect of vaccination with irradiated *Plasmodium yoelii* sporozoites on the repertoire of $\alpha\beta$ T lymphocytes in a murine model of malaria. Followed from Fig 113.

Fig 115: Effect of vaccination with irradiated *Plasmodium yoelii* sporozoites on the repertoire of $\alpha\beta$ T lymphocytes in a murine model of malaria. Followed from Fig 114.

Fig 116: Effect of vaccination with irradiated *Plasmodium yoelii* sporozoites on the repertoire of $\alpha\beta$ T lymphocytes in a murine model of malaria. Followed from Fig 115. (D) Group frequencies

Fig 117: Effect of vaccination with irradiated *Plasmodium yoelii* sporozoites on the repertoire of $\alpha\beta$ T lymphocytes in a murine model of malaria. Followed from Fig 116. (A-D) Group means & (D) Between group F matrix

Fig 118: Effect of vaccination with irradiated *Plasmodium yoelii* sporozoites on the repertoire of $\alpha\beta$ T lymphocytes in a murine model of malaria. Followed from Fig 117. (A) Between group F matrix (fold from Fig 117), Wilks lambda and Classification functions (A-D).

Fig 119: Effect of vaccination with irradiated *Plasmodium yoelii* sporozoites on the repertoire of $\alpha\beta$ T lymphocytes in a murine model of malaria. Followed from Fig 118. (B) Classification matrix; (C) Jackknifed classification matrix; (D) Eigen values; Canonical correlations ; Cumulative proportion of total dispersion ; Canonical discriminant functions

Fig 120: Effect of vaccination with irradiated *Plasmodium yoelii* sporozoites on the repertoire of $\alpha\beta$ T lymphocytes in a murine model of malaria. Followed from Fig 119.

Fig 121: Effect of vaccination with irradiated *Plasmodium yoelii* sporozoites on the repertoire of $\alpha\beta$ T lymphocytes in a murine model of malaria. Followed from Fig 120. (D) Canonical scores of group means.

Fig 122: Effect of vaccination with irradiated *Plasmodium yoelii* sporozoites on the repertoire of $\alpha\beta$ T lymphocytes in a murine model of malaria. Followed from Fig 121. (A) Canonical scores plots; (A-D) Clustering of discriminant factors.

Fig 123: Effect of vaccination with irradiated *Plasmodium yoelii* sporozoites on the repertoire of $\alpha\beta$ T lymphocytes in a murine model of malaria. Followed from Fig 122. (A) Cluster parallel coordinate plots; (B) Cluster profile plots.